Published in final edited form as:

Cerebellum. 2021 December ; 20(6): 836–852. doi:10.1007/s12311-021-01246-7.

Functional convergence of motor and social processes in lobule IV/V of the mouse cerebellum

Owen Y. Chao[1], **Hao Zhang**[1], **Salil Saurav Pathak**[1], **Joseph P. Huston**[2], **Yi-Mei Yang**[1,3,*]

[1]Department of Biomedical Sciences, University of Minnesota Medical School, Duluth, MN 55812, USA

[2]Center for Behavioral Neuroscience, Heinrich Heine University of Düsseldorf, Düsseldorf, Germany

[3]Department of Neuroscience, University of Minnesota, Minneapolis, MN 55455, USA

Abstract

Topographic organization of the cerebellum is largely segregated into the anterior and posterior lobes that represent its “motor” and “non-motor” functions, respectively. Although patients with damage to the anterior cerebellum often exhibit motor deficits, it remains unclear whether and how such an injury affects cognitive and social behaviors. To address this, we perturbed the activity of major anterior lobule IV/V in mice by either neurotoxic lesion or chemogenetic excitation of Purkinje cells in the cerebellar cortex. We found that both of the manipulations impaired motor coordination, but not general locomotion or anxiety-related behavior. The lesioned animals showed memory deficits in object recognition and social-associative recognition tests, which were confounded by a lack of exploration. Chemogenetic excitation of Purkinje cells disrupted the animals’ social approach in a less-preferred context and social memory, without affecting their overall exploration and object-based memory. In a free social interaction test, the two groups exhibited less interaction with a stranger conspecific. Subsequent *c-Fos* imaging indicated that decreased neuronal activities in the medial prefrontal cortex, hippocampal dentate gyrus, parahippocampal cortices and basolateral amygdala, as well as disorganized modular structures of the brain networks might underlie the reduced social interaction. These findings suggest that the anterior cerebellum plays an intricate role in processing motor, cognitive and social functions.

Keywords

cerebellum; lesion; chemogenetics; object recognition; social memory; functional connectivity

[*]**Correspondence to**: Yi-Mei Yang, PhD, Department of Biomedical Sciences, University of Minnesota Medical School, 1035 University Drive, Duluth MN 55812, USA, Phone: +1 218-726-7818, ymyang@d.umn.edu.

Author contributions

OYC and YMY designed the project, performed the experiments and analyzed the data. HZ and SSP contributed to data analysis and colony maintenance. JPH provided critical inputs and technical consultations. OYC, YMY, and JPH wrote the manuscript.

Conflict of interests

The authors declare no competing financial and non-financial interests.

Availability of data and materials

All the data are available upon request.

Introduction

The cerebellar cortex is folded into discrete lobules composed of the anterior (lobules I-V), posterior (lobules VI-IX) and flocculonodular (lobule X) regions [1]. Classically, each of the cerebellar divisions is viewed as a unit for executing a specific function ranging from sensorimotor to cognitive, affective and social behaviors [2–6]. In general, the anterior cerebellum preferentially interacts with the motor and somatosensory cortices, which is responsible for sensorimotor functions [1–6]. The posterior cerebellum particularly interacts with the prefrontal, parietal and temporal cortices, which subserves the processing of language, working memory and social cognition [1–6]. The functional separation is also found in patients with damage to the anterior cerebellum showing ataxic motor disability, while those with damage to the posterior cerebellum exhibiting cognitive and affective, but rarely motor, impairments [7–9]. The anterior and posterior lobes can be further divided into a central vermis, intermediate paravermis and lateral hemispheres [1]. The vermis and paravermis are connected to the limbic system [10], which can be activated during motor and emotional tasks [11–13]. Moreover, they are implicated in “non-motor” symptoms of autism [14], schizophrenia [15] and other psychiatric disorders [16, 17].

Social behaviors consist of complex processes, such as intentions, emotions and memories of encounters, which relate to social perception, interaction and recognition [18, 19]. The medial prefrontal cortex (mPFC), anterior cingulate cortex (ACC), orbitofrontal cortex (OFC), hippocampus, amygdala, temporal cortex and cerebellum are important areas recruited in the organization of social behaviors [6, 20–23]. The cerebellum projects to several nuclei, including the thalamus and ventral tegmental area (VTA), which further connect to all the aforementioned cortical regions that participate in social activities [24–26]. Optogenetic manipulation of the cerebellum was able to modulate motor, cognitive and social performances by influencing neuronal activities in the VTA, thalamus, motor cortex, mPFC and parietal association cortex [25, 27–29]. In addition, a study using functional magnetic resonance imaging (fMRI) revealed that optogenetic stimulation of the cerebellar cortex altered the activation of the ACC, hippocampus, primary motor cortex and retrosplenial cortex [30]. Chemogenetic inhibition of dopamine D1 receptor-positive neurons in the lateral cerebellar nucleus disrupted spatial navigation, working memory, response inhibition and social novelty [24]. Impaired social interaction is a common phenotype in neuropsychiatric disorders. Studies in autism illustrated that the cerebellar vermis and Crus I were critical neural correlates to autistic behaviors [14, 29, 31]. Noninvasive brain stimulation of the vermis produced therapeutic effects on patients with schizophrenia [32, 33]. Optogenetic stimulation of thalamic synaptic terminals of the cerebellar nucleus compensated abnormal neuronal firing in the mPFC and cognitive deficits in an animal model relevant to schizophrenia [28]. These lines of evidence suggest that by integrating into the cerebello-cerebral network, the cerebellum (mainly the posterior lobe) is causally linked to social functions [6]. However, it remains elusive whether and how the anterior cerebellum, a representation of sensorimotor control [34], contributes to social processing.

To this end, we manipulated the activity of major lobules (IV/V) in the mouse anterior cerebellar cortex either by a conventional neurotoxic lesion method (analogous to cerebellar injuries) or by a contemporary chemogenetic approach of increasing the excitability of the

output neurons, Purkinje cells (PCs) (analogous to cerebellar stimulation). Subsequently, we evaluated their impacts on mouse behaviors, including motor coordination, object recognition, social interaction and social memory. Following a free social interaction test, we conducted functional mapping of the cerebello-cerebral axis with an immediate early gene expression *c-Fos* [35]. Although both of the maneuvers impaired motor coordination and social interaction, the effects of the chemogenetic excitation of PCs, unlike the lesion, were not confounded by exploratory or motivational factors. This decoupling from the influence on the general activity supports the notion that the anterior cerebellum is engaged in social cognition.

Materials and Methods

Subjects

C57BL/6J mice were obtained from Jackson Laboratories (Bar Harbor, ME). They were grouped 3–5 per cage with free access to food and water. They were kept with controlled temperature and humidity under a light-dark cycle (light on from 7:00 to 19:00). They underwent the surgery (see below) at 6–8 weeks old. All procedures were in compliance with the Institutional Animal Care and Use Committee, University of Minnesota, and the Guide for the Care and Use of Laboratory Animals, National Institute of Health. As sex can be a potential variable, we only used male mice here to derive group differences. Future studies are needed to carefully examine sex difference by including male and female mice.

Surgery

Animals were randomly divided into 3 groups for microinjections of AAV5-hSyn-EGFP (control; n=10), N-Methyl-d-aspartate (NMDA; n=8) and AAV8-Pcp2-hM3Dq-mCherry (n=10). AAV5-hSyn-EGFP was purchased from Addgene (#50465, a gift from Dr. Bryan Roth). NMDA (M3262; Sigma-Aldrich, St. Louis, MO) is known to induce persistent lesions because of its neurotoxicity [36]. AAV8-Pcp2-hM3Dq-mCherry (titer $>4.0\times10^{13}$) was prepared by the University of Minnesota Viral Vector and Cloning Core following standard packaging procedures. Minimal Pcp2/L7 promoter was inserted into pAAV-CaMKIIa-hM3D(Gq)-mCherry (Addgene #50476, a gift from Dr. Bryan Roth) to confer specific expression of a human M3 muscarinic receptor (hM3Dq) to PCs (PC-M3) [31, 37]. The hM3Dq receptor can be activated by clozapine-*N*-oxide (CNO) to increase PC excitability, as attested in our laboratory [31]. Animals were anaesthetized with a cocktail of ketamine and xylazine (100 and 10 mg/kg, respectively, i.p.). Meloxicam (5 mg/kg, s.c.) was administrated as an analgesic. Animals were fixed on a stereotactic frame (Stoelting, Wood Dale, IL) and an incision was made to expose the skull. Holes were drilled above the cerebellum according to the coordinates: AP: −6.1 mm, ML: ±1.0 mm, relative to the bregma [38]. The viral vectors or NMDA solution (10 μg/μl in phosphate-buffered solution, PBS) were infused bilaterally into the cerebellum with a 33-gauge steel cannula inserted 1 mm below the dura via a 10 μl Hamilton syringe connected to a microinjection pump (CMA 100, Holliston, MA; 0.2 μl per side with a flowrate of 0.1 μl/min). After each infusion, the needle was left in place for >7 min and then slowly retracted. The wound was sutured and disinfected with 70% ethanol and iodine. Animals were placed on a heating pad (37°C) to maintain body temperature until awake. Behavioral testing was conducted 3 weeks later.

Animals were excluded (n=1–2/group) if the injection sites were outside the cerebellar lobule IV/V, according to the mouse brain atlas [38].

Apparatus

An elevated plus maze consisted of a central platform (5 × 5 cm), two walled arms (25 × 5 × 25 cm) and two arms without walls (25 × 5 cm) in the shape of a cross. It was elevated 30 cm high and the two types of arms were situated opposite to each other. A digital rotarod (Rotamex, Columbus Instruments, Columbus, OH) was used to test motor coordination. A transparent box (40 × 40 × 30 cm) made of polyvinyl chloride was used for open field, object recognition and social associative recognition tests. Different sets of objects with variable textures (smooth or rough), sizes (diameter 7–9 cm, height 14–17 cm) and shapes (column, irregular) were used for object recognition. The objects were weighed enough to prevent being moved by animals. Assignment of the objects was counterbalanced to minimize object and/or place preference. Metal grid cups (diameter 10 cm, height 12 cm) were used to constrain a stranger mouse for social-associative recognition and context-biased social tests. Placement of the stranger mouse was counterbalanced between subjects. A box contained three chambers (each 20 × 40 × 30 cm) was used for context-biased social tests. Different cues, black circles or horizontal stripes, were attached to either side of the box to make two distinct contexts. Animals could freely explore the box through passages (5 × 5 cm) between the chambers. A camera was set 1.5 m above and connected to a computer for tracking animals and recording videos with ANY-maze software (Stoelting). All tests were done in a sound-attenuated room (<40 decibels) under dim light (~50 lx) during 10:00–16:00. Apparatus was cleaned with 70% ethanol between animals.

Behavioral testing

As CNO metabolite clozapine *per se* could affect animal behaviors [39, 40], we controlled this factor by administrating CNO (Enzo Life Sciences, Farmingdale, NY) 30–40 min prior to each test in all the groups (1 mg/kg, i.p.). CNO was stored in aliquots at −20°C. Before use, CNO was diluted in saline (adjusted to the dose in a volume of 10 ml/kg), kept on ice and protected from light. Parameters for object exploration, social exploration and social interaction were counted by experimenters who were blind to the design. Other measurements were automatically made with the ANY-maze software. Durations of the tests were based on previous studies using similar experimental protocols [41–43] .

Elevated plus maze—This test was used to measure anxiety-like behavior [44]. The subject was placed onto the central platform (facing an open arm) and allowed to freely explore for 5 min. Distance travelled, time spent in the center, open and closed arms and entries into these areas were analyzed. A ratio (time spent in the open arms / time spent in the open and closed arms) was calculated to indicate anxiety levels.

Open field—This test was used to assess exploratory and locomotor activity. The subject was put into the center of the open field and tested for 10 min. Distance travelled, rearing, thigmotaxis, duration of grooming and travelling were analyzed. Rearing is a sign for non-selective attention [45]. Self-grooming is a measure of repetitive behavior [46]. Thigmotaxis is an index of sensorimotor function and/or anxiety [47, 48]. The test was conducted for

three consecutive days, while CNO was given on day 1 only. The tests on days 2–3 were served as a procedure of habituation to the open field before the object recognition and social associative recognition tests.

Rotarod—This test was used to evaluate motor coordination and motor learning. The subject was placed on the rotarod rotating at a constant speed of 4 rpm and it was ensured that the subject could stay on it for at least 1 min (all animals reached the standard). Then, the speed was accelerated from 4 to 40 rpm in 5 min, which was taken as one trial. Three trials were conducted with an inter-trial-interval of 15 min. Speed of rotation and duration of staying on the rotarod before falling were recorded.

Object recognition—This test was used to estimate object-based recognition memory [49, 50], composed of a learning trial and a test trial with an inter-trial-interval of 45 min. Two distinct objects were placed in the open field and the subject was allowed to freely explore them for 7 min in the learning trial. In the test trial, one of the objects was replaced with a novel object and the animal was given another 7 min to explore. Preference to the novel object over the familiar one indicated that the animal recognized the familiar object. Object exploration was defined as physical contacts to the object with the head, nose or forelimbs, but not other behaviors, such as climbing the object or sitting next to it.

Social associative recognition—This test was designed to assess social recognition memory, including a sociability trial, an association trial and a recognition trial, with inter-trial-intervals of 45 min. In the sociability trial, an age matched male C57BL/6J mouse (social stimulus), that was never encountered by the subject, was placed underneath a cup in the open field, along with another identical empty cup (non-social stimulus). The subject was then put into the arena and allowed to freely explore them for 7 min. Normal rodents explore the social stimulus more than the non-social one [31, 43]. In the association trial, two identical objects were placed in the same locations where the two cups previously occupied and the subject was allowed to explore for 7 min. More exploration of the object located in the previous “social” place implies the subject has formed an associative memory of which object is related to the stranger mouse. In the recognition trial, the same mouse used in the sociability trial was placed again underneath the cup, while a novel mouse (never contacted by the subject) was covered by the other cup. Locations of the cups and the previously contacted stranger were identical to the sociability trial. The subject was allowed to explore them for 7 min. More exploration of the novel stranger than the familiar one indicates that the subject recognizes the “contacted/familiar” stranger. Subjects that explored for less than 10 sec in either trial were excluded (n=1–2/group).

Context-biased social test—This test was designed to evaluate sociability in a challenging situation by presenting a stranger mouse in a less-preferred context. In the pre-test trial, the subject (drug-free) was placed into the middle chamber of the three-chambered box (neutral context) and was free to explore either side of the box with a distinct context for 15 min. Time spent in each chamber was recorded to determine the contextual preference (less versus more time spent in either context). Next day, a stranger mouse was placed underneath a cup located in the non-preferred side (less-preferred context),

while an identical empty cup was located on the other side (preferred context), based on the individual preference shown in the pre-test trial. In the test trial, the subject was administered CNO 30 min before being placed into the box and allowed to explore for 7 min. Time spent in each chamber and exploring the stranger or the empty cup were counted.

Free social interaction—This test was used to measure social behavior in a native situation without physical limitations. The subject was placed into the open field for 10 min together with another age matched male C57BL/6J mouse (stranger) that was never contacted by the subject. An interaction was defined as either part of the animal' head being in physical contacts with any body part of the other's, except for the tail. Behavioral subtypes, such as nose-to-nose/head (either animal's nose contacted the other's nose or head), nose-to-anogenital (either animal's nose contacted the base of the tail or anus of the other's), crawl over/under (either animal climbed over or below the other's back or abdomen) and following (either animal chased the other), were recorded. To map neurons activated by the free social interaction, all the groups were sacrificed 90 min after the test and used for *c-Fos* immunostaining (n=5–6/group, randomly chosen from each group). The 90-min time window was applied because *c-Fos* expression peaks 1–2 hours after stimulation [51].

Histology and immunohistochemistry

Mice were deeply anaesthetized, perfused with ice-cold PBS followed by 4% paraformaldehyde solution. The brain was removed, immersed in 4% paraformaldehyde solution at 4°C overnight, transferred into 30% sucrose solution and stored at 4°C until processed. The cerebellum was dissected out for examining the extent of lesions and the distribution of fluorescent proteins. Therefore, it was not used for *c-Fos* immunostaining. The brain was coronally sectioned into 40 μm-thick slices with a microtome (Leica SM2010 R, Buffalo Grove, IL). Slices were cover-slipped with a mounting medium containing DAPI (H-1200, Vector Lab, Burlingame, CA), and imaged with a Zeiss LSM 710 confocal microscope. Cell presence was identified by DAPI positive signals.

For *c-Fos* immunostaining, brain sections were pretreated with 0.3% H_2O_2 PBS for 10 min and incubated in blocking solution (2% goat serum and 0.2% Triton X-100 in PBS) at 37°C for 30 min. They were then incubated in blocking solution containing a primary antibody (1:2000, rabbit anti-*c-Fos*, ab190289, Abcam, Cambridge, MA) at 4°C for 24–48 h. They were washed with 0.2% Triton X-100 and incubated with biotinylated anti-rabbit IgG (1:200, BA-1000, Vector Lab) at room temperature for 2 h. After being washed with 0.2% Triton X-100, they were incubated for 1 h in the ABC kit (PK-4000, Vector Lab) and 3,3' diaminobenzidine chromogen (for visualization). They were cover-slipped with a mounting medium (H-5000, Vector Lab) and imaged with a Leica DMi8 light microscope under a 10x lens. Brain regions were identified according to a mouse brain atlas [38]. Experimenters who were blind to the design counted the number of *c-Fos*-positive cells with ImageJ (NIH). Each brain region was counted bilaterally across 2–4 consecutive sections. To minimize variability, the number of *c-Fos*-positive cells in each group was divided by the average value of the control group within the same region and defined as fold change.

Interregional *c-Fos* correlations and graph theoretical analysis

Matrices of correlation were created by calculating Pearson coefficients (r) from the number of *c-Fos*-positive cells inter-regionally within each group. Pearson coefficients were Fisher z-transformed and statistics was conducted to compare average values between groups. Positive and negative r were color-coded in red and indigo respectively in a gradient spectrum. Each node represented a brain region and each connecting line represented the Pearson correlation between regions.

Graph theoretical analysis was performed to identify properties of the brain networks activated by free social interaction. The networks were constructed by unweighted adjacency matrices for each group produced by significant (uncorrected $p<0.1$) and positive correlations ($r>0.7$) of interregional *c-Fos* counts. Due to a small size of the networks (12 nodes in total), we here chose $p<0.1$ over $p<0.05$ as statistical significance to preserve interregional connections derived from the graph theoretical analysis. Although this might overestimate the network structures, we opted for a strict r value (>0.7) to control the mathematical modeling error. Graph theoretical indices of degree and betweenness were calculated to reveal network centrality, which denotes the number of edges/connections that are incident to the node and the number of shortest paths that pass through the node, respectively. Within-module Z-scores (a measure of the degrees of a given node connecting with other nodes in the community; intramodule connectivity) and participation coefficient (a measure of the diversity of each node's connections across the network's communities; intermodule connectivity) were determined for the brain regions in the networks. Clusters/modules which optimized the modularity through enumeration of all potential community structures were identified. Graph theoretical analysis was conducted in MATLAB (R2015b) with the Brain Connectivity Toolbox (https://sites.google.com/site/bctnet/). Calculation details were described previously [52–54].

Statistics

Mixed two-way ANOVAs with between factors ("group") and within factors ("object" or "trial") were applied to analyze behaviors. One-way ANOVAs were applied to analyze *c-Fos* and behavior data when appropriate. Paired t-tests, independent t-tests and Mann-Whitney U tests (if disobeying homogeneity or normality of variance) were used when main effects were revealed. The lesion and the PC-M3 groups were compared to the control animals, separately. All analyses were two-tailed statistics with p set <0.05. Values were expressed as mean ± standard error of mean (SEM).

Results

Selective targeting of cerebellar lobule IV/V

To examine the efficacy of NMDA-induced lesions and AAV-mediated transduction of hM3Dq and/or fluorescent proteins, the cerebellar slices were imaged several weeks after surgical infusions and behavioral tests (Fig. 1a). The cerebellar cortex comprises three well-defined layers: the granular layer (GL), Purkinje cell layer and molecular layer (ML) [1]. We found that in the control group EGFP was present in all types of neurons within lobule IV/V, with a majority of expression in granule cells and interneurons (Fig. 1b). This

is expected as AAV5-hSyn-EGFP can induce neuron-specific but not neuronal type-specific expression [55]. In the lesioned group, the damage was localized in lobule IV/V as reflected by a lack of clear structure of the cerebellar layers (Fig. 1b). Presumably all the cells in the region were lost [36]. The PC-M3 group exhibited robust expression of hM3Dq (visualized with mCherry) selectively in PCs of lobule IV/V, covering the soma, dendrites and axons of PCs (Fig. 1b). This is consistent with our early report on the efficiency and specificity of AAV8-Pcp2-hM3Dq-mCherry in targeting PCs with the help of a Pcp2 promoter [31]. Fig. 1c illustrated a coronal view of the distribution of NMDA-induced lesions and AAV-mediated transductions near the vermis (bilateral paravermis) along the rostral-caudal axis. We quantified the affected area by normalizing it to the total area of lobule IV/V across the sections, and noticed that 33.6 ± 9 %, 26.1 ± 8 % and 18.4 ± 5 % of lobule IV/V were targeted in the control (n=9), lesion (n=7) and PC-M3 (n=9) groups, respectively.

Effects of manipulation of lobule IV/V on anxiety-related behavior, locomotor activity, motor coordination and object memory

One-way ANOVA tests of mouse behavior on the elevated plus maze did not show significant “group” effects in all the measured parameters ($p>0.05$), except for time spent in the center ($F_{2, 22}=4.263$, $p=0.027$; Fig. 2a). A further analysis of the time spent in the center with independent *t*-tests did not reveal a significant difference for the lesion or the PC-M3 group when compared to the control group, separately ($p>0.05$). Overall, similar levels of anxiety were found among all the cohorts.

In the open field, there were significant “group” effects in thigmotaxis ($F_{2, 21}=3.641$, $p=0.044$) and duration of grooming ($F_{2, 21}=7.515$, $p=0.003$), but not in distance travelled, rearing and duration of travelling ($p>0.05$; Fig. 2b). A following analysis of thigmotactic behavior failed to detect any significant differences between the lesion, PC-M3 and control groups ($p>0.05$, independent *t*-tests). Interestingly, the lesion, but not the PC-M3, group spent more time on self-grooming than the control animals did ($t_{14}=3.093$, $p=0.008$). Thus, while general locomotor activities were not affected by either of the manipulations, the neurotoxic lesion, but not chemogenetic excitation of PCs, in lobule IV/V, induced excessive repetitive behavior [46].

In the rotarod test, there were significant effects of “group” ($F_{2, 21}=5.78$, $p=0.01$) and “trial” ($F_{2, 42}=8.651$, $p=0.001$), but not “group × trial” interaction ($p>0.05$), in the analysis of time stayed on the rotarod (Fig. 2c). Neither the lesion ($F_{1,14}=6.529$, $p=0.023$) nor the PC-M3 ($F_{1,15}=7.144$, $p=0.017$) group stayed as long as the control group (repeated one-way ANOVAs, separately). Similarly, significant effects of “group” ($F_{2, 21}=5.901$, $p=0.009$) and “trial” ($F_{2, 42}=8.765$, $p=0.001$), but not their interaction ($p>0.05$), were found in the analysis of maximal speed reached before falling. The lesion ($F_{1,14}=6.899$, $p=0.02$) and PC-M3 ($F_{1,15}=6.97$, $p=0.019$) groups attained lower speed than the control group. The results suggest that both of the maneuvers in lobule IV/V led to deficits in motor coordination.

In the object recognition test, there were significant effects of “group” ($F_{2, 17}=12.822$, $p<0.001$), “object” ($F_{1, 17}=26.744$, $p<0.001$) and “group × object” ($F_{2, 17}=9.576$, $p=0.002$), in the analysis of object exploration (Fig. 2d). As the main effect of “group × object” or “object” was found, paired *t*-tests were used within each group, separately. The

control (t_7=−2.498, p=0.041) and PC-M3 (t_6=−5.217, p=0.002) groups, but not the lesion group (p>0.05), explored the novel object more than the old one, indicating intact object recognition. One-way ANOVA revealed significant effects of "group" in the analysis of distance traveled and total object exploration time in the learning ($F_{2, 18}$=4.864, p=0.02; $F_{2, 18}$=7.192, p=0.005, respectively) and in the test ($F_{2, 18}$=8.484, p=0.003; $F_{2, 17}$=12.822, p<0.001, respectively) trials. The lesion group showed less distance travelled and total exploration than the control group in the learning (t_{12}=3.152, p=0.008; t_{12}=3.447, p=0.005, respectively) and in the test (t_{12}=4.853, p<0.001; t_{12}=4.137, p=0.001, respectively) trials. By contrast, the PC-M3 group did not exhibit such differences when compared to the control mice in all the trials (p>0.05). Taken together, the neurotoxic lesion in lobule IV/V impaired animals' novel object preference, which was likely confounded by their deficient motivation and/or attention, whereas the chemogenetic excitation of PCs did not compromise the object recognition memory.

Perturbation of lobule IV/V disrupted social memory and social interaction

The social associative recognition test was designed to understand the complexity of social behaviors including social approach, social association and social memory. In the sociability trial, significant effects of "group" ($F_{2, 19}$=5.48, p=0.013) and "object" ($F_{1, 19}$=60.212, p<0.001), but not their interaction (p>0.05), were found in the analysis of exploration performance. All the groups showed a preference for the stranger over the empty cup (control, t_7=8.619, p<0.001; lesion, t_6=5.822, p=0.001; PC-M3, t_6=2.779, p=0.032), suggestive of intact social approach (Fig. 3a(i)). In this trial, there was a significant "group" effect in total exploration ($F_{2, 19}$=5.48, p=0.013), but not in distance travelled (p>0.05). Overall, the lesion group explored less than the control group (t_{13}=2.273, p=0.041), while the PC-M3 group did not (p>0.05). In the association trial, there were significant effects of "group" ($F_{2, 19}$=7.042, p=0.005) and "object" ($F_{1, 19}$=12.971, p=0.002), but "group × object" interaction (p>0.05) in the analysis of object exploration. The control group explored the socially associated object more than the non-associated one (t_7=3.954, p=0.006), while the lesion and PC-M3 groups did not (p>0.05), indicating impaired social associative memory by the interfering of lobule IV/V (Fig. 3a(ii)). Moreover, significant "group" effects were found in the analysis of distance travelled ($F_{2, 19}$=6.617, p=0.007) and total exploration ($F_{2, 19}$=7.042, p=0.005). The lesioned animals travelled and explored less than the controls (t_{13}=3.469, p=0.004; t_{13}=4.828, p<0.001, respectively), in line with the finding in the object recognition test (Fig. 2d). Yet, the PC-M3 animals were not different from the control group in distance travelled or total exploration (p>0.05). In the recognition trial, there were significant effects of "group" ($F_{2, 19}$=4.761, p=0.021) and "group × object" ($F_{2, 19}$=5.728, p=0.011), but not "object" (p>0.05), in the analysis of exploratory behavior. The control group explored the novel stranger more than the familiar one (t_7=−3.867, p=0.006), but the lesion and PC-M3 groups did not (p>0.05), implying defective social recognition following the perturbation of lobule IV/V (Fig. 3a(iii)). Additionally, there was a significant effect of "group" in the analysis of total exploration ($F_{2, 19}$=4.761, p=0.021), but not distance travelled (p>0.05). The lesioned mice showed less exploration than the controls (t_{13}=2.21, p=0.046), whereas the PC-M3 group did not differ from the controls in total exploration (p>0.05). Collectively, although both NMDA-induced lesion and chemogenetic excitation of PCs in lobule IV/V disrupted social association and recognition memory,

the underlying mechanisms might be different. The performance of the lesion group was highly compromised by their low motivation and exploration levels. However, the behavior of the PC-M3 animals was unlikely influenced by these factors as their general motor and exploratory activities were comparable to the control group, which reinforced the engagement of the anterior cerebellum in social behaviors.

As all the groups showed intact sociability (Fig. 3a(i)), we challenged them with the context-biased social test. In the pre-test trial, all the groups stayed in one of the contexts longer than the other (control, $t_7=-4.255$, $p=0.004$; lesion, $t_6=-2.912$, $p=0.027$; PC-M3, $t_7=-3.482$, $p=0.01$), suggesting that they were able to differentiate the contexts and form a natural contextual preference (Fig.3 b(i)). In the test trial, significant effects of "group" ($F_{2,20}=11.512$, $p<0.001$) and "object" ($F_{1,20}=17.67$, $p<0.001$), but not their interaction, were found in the analysis of exploration. The control ($t_7=5.662$, $p<0.001$) and lesioned ($t_6=3.73$, $p=0.01$) animals explored the stranger located in the non-preferred context more than the empty cup located in the preferred context, but the PC-M3 group did not ($p>0.05$; Fig. 3b(ii)). A further scrutiny of the PC-M3 animals confirmed that they did not have a strong preference for the social stimulus across the time periods of the test ($p>0.05$). There was a significant effect of "group" in the analysis of total exploration ($F_{2,20}=11.512$, $p<0.001$), but not distance travelled ($p>0.05$; Fig. 3b(iii–iv)). The lesion ($t_{13}=4.176$, $p=0.001$) and PC-M3 ($t_{14}=4.45$, $p<0.001$) groups had higher total exploration than the control group. No differences were found in time spent in each chamber ($p>0.05$), except that the lesion group stayed longer in the center chamber than the controls ($t_{13}=3.093$, $p=0.009$; Table 1). Despite that the exploratory behavior appeared to be facilitated by the manipulations of lobule IV/V under the condition of combined contextual and social stimuli, chemogenetic excitation of PCs specifically weakened the animals' social approach in the challenging situation.

In the free social interaction test, one-way ANOVA revealed a significant "group" effect in the duration of interaction ($F_{2,21}=30.59$, $p<0.001$). The lesion ($t_{13}=4.492$, $p<0.001$) and PC-M3 ($t_{15}=7.122$, $p<0.001$) groups spent less time on social interaction than the control mice (Fig. 4a). In the analysis of frequencies of nose-to-nose/head, nose-to-anogenital, crawl-over/under and following, significant "group" effects were found for all the parameters (nose-to-nose/head, $F_{2,21}=6.942$, $p=0.005$; crawl-over/under, $F_{2,21}=16.324$, $p<0.001$; following, $F_{2,21}=15.083$, $p<0.001$) except for nose-to-anogenital ($p>0.05$). The lesion group displayed a higher frequency of nose-to-nose/head than the control group ($t_{13}=3.763$, $p=0.002$). The lesion and PC-M3 groups showed lower frequencies of crawling-over/under ($t_{13}=3.082$, $p=0.009$ and $t_{15}=4.817$, $p<0.001$, respectively) and following ($t_{13}=3.353$, $p=0.005$ and $t_{15}=4.667$, $p<0.001$, respectively) than the control group (Fig. 4a). The results indicate that perturbing lobule IV/V decreased animals' social activities when they encountered a freely behaving stranger. Behavior results from the manipulations in the cerebellar lobule IV/V are summarized in Table 2.

Interference of lobule IV/V disorganized brain network structure for free social interaction

To understand how the anterior cerebellar lobules are involved in social behaviors, we probed the brain network activity 90 min after the free social interaction test by immunostaining the protein product of an immediate early gene, *c-Fos*, as a marker for

neuronal activity [35]. The 90-min time window was applied because *c-Fos* expression peaks 1–2 hours after stimulation [51]. Fig. 4b illustrated diagrams of brain regions where *c-Fos*-positive cells were imaged and counted. They were the mPFC subregions (prelimbic cortex, PL; infralimbic cortex, IL), OFC, ACC, dorsal hippocampal subregions (CA1, CA3 and dentate gyrus, DG), dorsal retrosplenial cortex (RSD), parietal association cortex (PtA), entorhinal cortex (Ent), perirhinal cortex (Prh) and basolateral amygdala (BLA). These regions were selected because of their well-known functions in social behaviors [20, 21, 56–58].

In the analysis of fold changes of *c-Fos*, there were significant "group" effects for the regions PL ($F_{2, 14}$=4.847, p=0.025), IL ($F_{2, 14}$=29.008, p<0.001), ACC ($F_{2, 14}$=23.864, p<0.001), CA1 ($F_{2, 14}$=4.097, p=0.04), DG ($F_{2, 14}$=5.626, p=0.016), RSD ($F_{2, 14}$=8.24, p=0.004), PtA ($F_{2, 14}$=12.214, p=0.001), Prh ($F_{2, 14}$=5.074, p=0.022) and BLA ($F_{2, 14}$=51.086, p<0.001), but not OFC, CA3 and Ent (p>0.05). Compared to the control group, the *c-Fos* levels in all the regions, except in the CA1 (p>0.05), were reduced in the lesion group (PL: U=4, p=0.052 [marginally significant]; IL: U=0, p=0.004; ACC: U=0, p=0.004; DG: U=3, p=0.03; RSD: U=2, p=0.017; PtA: U=2, p=0.017; Prh: U=3, p=0.03; BLA: U=0, p=0.004) and in the PC-M3 group (PL: U=0, p=0.004; IL: U=0, p=0.004; ACC: U=0, p=0.004; DG: U=2, p=0.017; RSD: U=3, p=0.03; PtA: U=1, p=0.009; Prh: U=4, p=0.052 [marginally significant]; BLA: U=0, p=0.004; Mann-Whitney U tests) (Fig. 4c). The decrease in *c-Fos* expression was in accordance with the impaired free social interaction by the perturbations of lobule IV/V (Fig. 4a).

Matrices of interregional correlations for each group were depicted in Fig. 4d. The Pearson's r from 1 to −1 was color-coded in red and indigo respectively in a gradient spectrum. Network graphs were constructed with the brain regions (nodes) and their connections (edges; significant interregional correlations), based on their *c-Fos* expression. The positive (r>0.7) and negative (r<−0.7) correlations were shown in solid and dashed lines, respectively. The control group had more edges with proportionally more positive correlations than the lesion or the PC-M3 group (pie charts in Fig. 4d). One-way ANOVA confirmed that there was a significant "group" effect in the mean r values ($F_{2, 195}$=8.223, p<0.001). The r values for the lesion (t_{130}=3.989, p<0.001) and PC-M3 (t_{130}=2.366, p=0.019) groups were lower than that for the control group, implicating that the manipulations of lobule IV/V disorganized the brain-wide interregional connectivity required for free social interaction.

We performed graph theoretical analysis to characterize the neural networks by focusing on the positive correlations of the matrices for each group. The graph theoretical parameters, degree (the number of edges of a given node) and betweenness (the number of shortest paths passing through a given node), were calculated. The control and PC-M3 groups had higher ranks of degree in the DG and IL and higher ranks of betweenness in the IL, whereas the lesion group showed higher ranks of degree and betweenness in the BLA and Ent (Fig. 5). The community structure of the networks for each group was built upon the within-community Z-scores (the extent of a node connected within its own community) and participation coefficients (the extent of a node connected to other communities) [53]. If a node (brain region) has a higher value of both within-community Z-score and participation

coefficient, it is considered as a key hub in the modulation of the interactions between disparate parts of a network [59]. In the control group, two major modules were identified, namely IL and RSD, as the functional hubs mediating free social interaction (Fig. 5). The IL module, including the mPFC, hippocampus and BLA, is known for cognitive, mnemonic and emotional processing [50, 60]. The RSD module, containing the parahippocampal cortices and CA3, may play a role in integrating multiple sensory information for memory establishment in the hippocampus [61, 62]. These modules were not formulated in the lesion and PC-M3 groups. Instead, the lesion group had a module of parahippocampal cortices and BLA; and the PC-M3 group had a less organized ("weaker") module, IL and parahippocampal cortices-DG (Fig. 5). These findings suggest that the lesions in lobule IV/V interrupted the social interaction network "in quality" as the presence of the Ent-BLA module might alter sensory integration, memory and emotion, whereas the chemogenetic excitation disrupted the modular organization of the network "in quantity". It should be noted with caution that the values of participation coefficient for the two groups were zero, and thus, they did not form >1 module by the analysis. Yet, it was clear that the interference of the anterior cerebellum destructed the modular structure of brain networks for free social interaction.

Discussion

Our results demonstrate that perturbation of lobule IV/V in the cerebellum impairs animals' motor coordination, social memory and social interaction, but not general locomotion or anxiety. For the NMDA-induced lesion group, the impaired social memory and social interaction were likely confounded by a lack of motivation or attention to the stimuli, as manifested by the changes in total exploration and motor activity. However, the social deficits caused by the chemogenetic excitation of PCs were unlikely attributed to these factors as they were comparable to the control group. This new approach of interfering the cerebellar activity has provided supporting evidence for an intricate role of the anterior cerebellum in social behaviors. Furthermore, *c-Fos* functional mapping shows that the anterior cerebellum is an essential component in the cerebello-cerebral pathway enabling free social interaction.

In agreement with the classical view on the functionality of the anterior cerebellum [63, 64], our manipulation of lobule IV/V, either by lesion, or by increasing PC firing, resulted in an impairment in the coordination of delicate and adaptable movements (Fig. 2c). The result from the distinct types of manipulation further confirms that the accurate output information from the cerebellar cortex is important for motor control [65]. Meanwhile, the localized perturbations did not alter basic motor activity in non-challenging conditions, *e.g.*, in the open field test (Fig. 2b). Interestingly, lesion of lobule IV/V generated the stereotyped behavior of self-grooming. Excessive grooming is a characteristic feature in animal models for studying psychiatric disorders, including autism and obsessive-compulsive disorder [46]. For example, in an autistic-like mouse model, we have shown that excessive grooming can be rectified by selectively boosting the excitability of PCs [31]. The lesioned animals also exhibited less exploration in the object- and social-memory tests (Fig. 2d & 3a), which may reflect the deficits in motivation/attention or sensorimotor function. The latter is compatible with the perspective that the anterior cerebellum modulates sensorimotor integration [27] by

connecting to the sensory and motor systems [66, 67]. Clinical evidence corroborates that patients with injuries in the anterior cerebellum dominantly show motor defects [7–9].

By contrast, the chemogenetic manipulation did not have such an effect on overall exploration (Fig. 2–3). A possible explanation is that the method was designed to elevate the output activity of lobule IV/V [31], opposite to the intended outcome of the neurotoxic lesions [36]. Thereby, this operation was able to isolate the “cognitive” and “social” aspects of the anterior cerebellum from other perplexing variables, including anxiety (Fig. 2). The posterior vermis/paravermis is extensively connected to the limbic system for processing affective information [11–13]. The lack of effect on anxiety-relevant behavior following the perturbation of the anterior counterpart (lobule IV/V) may relate to its different anatomical organizations with the cerebrum, and/or the limited alterations made by this approach.

Social behaviors rely on social perception, interaction and recognition [18, 19]. Although the interpretation of social approach itself is vague due to its involvement in affiliative, territorial or aggressive behaviors [68, 69], the fact that the lesion and PC-M3 groups explored the stranger mouse more than the empty cup during the sociability trial suggests that they had intact discrimination and preference between social and non-social stimuli (Fig. 3a). Interestingly, the social approach of the PC-M3 animals diminished when the stranger was placed in a less-preferred context, despite that they showed a higher level of total exploration (Fig. 3b). Since the stranger, a naturally preferred stimulus, was located in the less-preferred context, the combined stimuli could cause a conflict in information handling, which seemed to be exacerbated by the cerebellar disturbance. This may be interpreted as such that the conflict response processed in the PFC [70, 71] interacts with the cerebellum-dependent motor planning [72] to decide which side to visit in the context-biased social test. It is also possible that the chemogenetic maneuver amplified the animals’ contextual preference. Future studies are required to test the hypotheses. Memory capacity is another prerequisite for normal social behaviors. The PC-M3 group showed intact object recognition (Fig. 2d), precluding the possibility that they lacked recognition memory in general. Thus, the impaired social memory in this group (Fig. 3a) is likely accounted by the detriments in social association and/or social recognition *per se*.

In the free social interaction test, nose-to-nose or nose-to-anogenital contacts were unchanged in the PC-M3 group (Fig. 4a), implying the animals had the intact ability to “identify” the stranger with their nose. However, the lesion group had slightly more nose-to-nose contacts with the stranger, which may indicate a sensory defect (taking an extra effort to “identify” a conspecific). Both of the groups showed less crawling and following the stranger, which can serve as signs of flawed social play [73, 74] or reduced territorial and aggressive behavior [75]. Nevertheless, the decrease in overall physical contacts suggests a deficiency in properly “reacting” to the conspecific as a result of the cerebellar perturbations.

Following the free social interaction test, we conducted *c-Fos* functional mapping of the brain networks activated by the native social acting. We found that the cerebellar lobule IV/V were essential for coordinating the networks of mPFC, hippocampus and amygdala in the processing of social information (Fig. 4–5). The identified mPFC-hippocampus-BLA

and parahippocampal-hippocampus modules may represent social conceptual information and multi-sensory information integrated into the hippocampal memory system, respectively. As a hub, the IL interacts with the hippocampus and amygdala to control cognition and emotion [60, 76]. The RSD being another hub functions to encode the context-specific ensembles [61], in association with episodic memory [62]. The susceptibility of these two modules to the manipulations of lobule IV/V implicates that the anterior cerebellum influences social interaction through the cerebello-cerebral axis. Since sensorimotor is a necessary component of free social interaction, the network structure inevitably embeds the processing of sensory and motor information. The shifted module in the lesion group (the parahippocampal cortices and BLA) may represent a functional compensation in light of the close relationship of cerebellar vermis-limbic system [10] , whereas the chemogenetic PC excitation did not produce such a shift, probably because of its minimal impact on the exploratory activity (Fig. 2–3). In spite of being a validated tool to detect activated neurons, *c-Fos*-based functional mapping has limitations. For instance, it has low temporal resolution as *c-Fos* expression is a slow transcriptional consequence of behavioral induction [51]. Therefore, it cannot provide real-time measurements of neuronal activity. Future investigations using multichannel *in vivo* electrophysiology, Ca^{2+} imaging and fMRI are needed to address how certain populations of neurons become simultaneously active in a task-related manner with temporal precision. Although *c-Fos* is commonly viewed as a marker for neuronal activation, the basal level of *c-Fos* in the brain is low [77] and an increase of *c-Fos* is not simply due to enhanced firing activity of neurons but requires changes in afferent inputs [78], implying a degree of specificity of *c-Fos* to external stimuli. Even so, other factors such as stress and pain can affect *c-Fos* expression. The conceptualized network model of social interaction built upon *c-Fos* labelling shall be taken with caution (Fig. 5). Nevertheless, to minimize the variables, we conducted the free social interaction test in the same condition for all the groups and normalized the *c-Fos* counts to the average value of the control group for each brain region. Thereby, the structural breakdown of the networks may largely result from the cerebellar interventions.

The different behavior phenotypes associated with the lesion and PC-M3 groups can be explained by the obvious distinctions between the two manipulations (Fig. 2b, 2d & 3b). Exposure to NMDA leads to permanent damage and presumably decreases the output from the cerebellar cortex [36], whereas chemogenetic excitation of PCs transiently increases the output activity upon CNO administration [31, 37]. Yet, it is unclear how the different maneuvers generated similar deficits in motor coordination (Fig. 2c) and social behaviors (Fig. 3a & 4a). As discussed earlier, this may indicate that the precise cerebellar output information is crucial for executing these functions [65]. It may also relate to potential effects outside the targeted region due to functional reorganization of brain circuits and compensation from non-transduced or non-injured PCs. It is worth noting that similar behavior manifestations are not necessarily mediated by the same neural basis. For example, both of the operations reduced free social interaction but yielded different network structures (Fig. 4 & 5).

It is well accepted that the posterior cerebellum acts as a primary mediator for social cognition [6]. Neuroimaging studies have pinpointed the double motor (lobules I-VI and VIII) and triple non-motor (lobules VI/Crus I, Crus II/VIIB and IX/X) representations in

the topographic arrangement [79, 80]. Although our current finding of the anterior lobule IV/V underlying social behavior seems surprising, it is resonant with recent evidence that lobule IV/V are associated with hippocampus-dependent object location memory [81], and attention and working memory [82]. Within the scope of this study, we cannot ensure that the behavioral outcomes exclusively resulted from the dysfunctions of the anterior cerebellum because our manipulations might have affected other lobules via the cerebellar intrinsic circuitry or extensive reciprocal projections between the cerebellum and other brain areas [1]. Future inquiries, for instance, with anatomical tracing, will establish comprehensive structural and functional networks that enable the intricate functions of the anterior cerebellum.

Conclusion

We uncover a complex role of the anterior cerebellum in converging motor and social functions. Knowing that the cerebellum is broadly involved in motor, neurodevelopmental and neuropsychiatric disorders [83–86], our findings may help develop novel strategies for their clinical interventions.

Acknowledgements

AAV8-Pcp2-hM3Dq-mCherry was generated by Dr. Ezequiel Marron Fernandez de Velasco in the University of Minnesota Viral Vector and Cloning Core with a plasmid from Addgene (a gift from Dr. Bryan Roth). AAV5-hSyn-EGFP was purchased from Addgene (a gift from Dr. Bryan Roth). We thank Dr. Matthew Slattery in our department for his invaluable inputs.

Funding information

This study was supported by the National Institute of Neurological Disorders and Stroke (NINDS) of the National Institutes of Health (NIH) grant R15NS112964 to YMY, the Winston and Maxine Wallin Neuroscience Discovery Fund to YMY, and the University of Minnesota faculty start-up fund to YMY. We also appreciate funding support from the DFG to JPH (HU 306/27-3).

References

1. Purves D, et al., Neuroscience. 2019.
2. Koziol LF, et al. , Consensus paper: the cerebellum’s role in movement and cognition. Cerebellum, 2014. 13(1): p. 151–77. [PubMed: 23996631]
3. Sokolov AA, Miall RC, and Ivry RB, The Cerebellum: Adaptive Prediction for Movement and Cognition. Trends Cogn Sci, 2017. 21(5): p. 313–332. [PubMed: 28385461]
4. Sathyanesan A, et al. , Emerging connections between cerebellar development, behaviour and complex brain disorders. Nature Reviews Neuroscience, 2019. 20(5): p. 298–313. [PubMed: 30923348]
5. Schmahmann JD, et al. , The Theory and Neuroscience of Cerebellar Cognition. Annu Rev Neurosci, 2019. 42: p. 337–364. [PubMed: 30939101]
6. Van Overwalle F, et al. , Consensus paper: cerebellum and social cognition. Cerebellum, 2020.
7. Schmahmann JD, Macmore J, and Vangel M, Cerebellar stroke without motor deficit: clinical evidence for motor and non-motor domains within the human cerebellum. Neuroscience, 2009. 162(3): p. 852–61. [PubMed: 19531371]
8. Deluca C, et al. , The cerebellum and visual perceptual learning: evidence from a motion extrapolation task. Cortex, 2014. 58: p. 52–71. [PubMed: 24959702]
9. Stoodley CJ, et al. , Location of lesion determines motor vs. cognitive consequences in patients with cerebellar stroke. Neuroimage Clin, 2016. 12: p. 765–775. [PubMed: 27812503]

10. Blatt GJ, Oblak AL, and Schmahmann JD, Cerebellar Connections with Limbic Circuits: Anatomy and Functional Implications, in Handbook of the Cerebellum and Cerebellar Disorders, Manto M, et al., Editors. 2013, Springer Netherlands: Dordrecht. p. 479–496.
11. Stoodley CJ and Schmahmann JD, Functional topography in the human cerebellum: a meta-analysis of neuroimaging studies. Neuroimage, 2009. 44(2): p. 489–501. [PubMed: 18835452]
12. Baumann O and Mattingley JB, Functional topography of primary emotion processing in the human cerebellum. Neuroimage, 2012. 61(4): p. 805–11. [PubMed: 22465459]
13. Keren-Happuch E, et al. , A meta-analysis of cerebellar contributions to higher cognition from PET and fMRI studies. Hum Brain Mapp, 2014. 35(2): p. 593–615. [PubMed: 23125108]
14. Khan AJ, et al. , Cerebro-cerebellar resting-state functional connectivity in children and adolescents with autism spectrum disorder. Biol Psychiatry, 2015. 78(9): p. 625–34. [PubMed: 25959247]
15. Ichimiya T, et al. , Reduced volume of the cerebellar vermis in neuroleptic-naive schizophrenia. Biol Psychiatry, 2001. 49(1): p. 20–7. [PubMed: 11163776]
16. Schmahmann JD and Sherman JC, The cerebellar cognitive affective syndrome. Brain, 1998. 121 (Pt 4): p. 561–79. [PubMed: 9577385]
17. Schmahmann JD, The role of the cerebellum in affect and psychosis. Journal of Neurolinguistics, 2000. 13(2–3): p. 189–214.
18. Frith CD and Frith U, Mechanisms of social cognition. Annu Rev Psychol, 2012. 63: p. 287–313. [PubMed: 21838544]
19. Pavlova MA, Biological motion processing as a hallmark of social cognition. Cereb Cortex, 2012. 22(5): p. 981–95. [PubMed: 21775676]
20. Adolphs R, The neurobiology of social cognition. Curr Opin Neurobiol, 2001. 11(2): p. 231–9. [PubMed: 11301245]
21. Amodio DM and Frith CD, Meeting of minds: the medial frontal cortex and social cognition. Nat Rev Neurosci, 2006. 7(4): p. 268–77. [PubMed: 16552413]
22. Bzdok D, et al. , Segregation of the human medial prefrontal cortex in social cognition. Front Hum Neurosci, 2013. 7: p. 232. [PubMed: 23755001]
23. Van Overwalle F, et al. , Social cognition and the cerebellum: a meta-analysis of over 350 fMRI studies. Neuroimage, 2014. 86: p. 554–72. [PubMed: 24076206]
24. Locke TM, et al. , Dopamine D1 receptor-positive neurons in the lateral nucleus of the cerebellum contribute to cognitive behavior. Biol Psychiatry, 2018.
25. Carta I, et al. , Cerebellar modulation of the reward circuitry and social behavior. Science, 2019. 363(6424).
26. Badura A, et al. , Normal cognitive and social development require posterior cerebellar activity. Elife, 2018. 7.
27. Proville RD, et al. , Cerebellum involvement in cortical sensorimotor circuits for the control of voluntary movements. Nat Neurosci, 2014. 17(9): p. 1233–9. [PubMed: 25064850]
28. Parker KL, et al. , Delta-frequency stimulation of cerebellar projections can compensate for schizophrenia-related medial frontal dysfunction. Mol Psychiatry, 2017. 22(5): p. 647–655. [PubMed: 28348382]
29. Stoodley CJ, et al. , Altered cerebellar connectivity in autism and cerebellar-mediated rescue of autism-related behaviors in mice. Nat Neurosci, 2017. 20(12): p. 1744–1751. [PubMed: 29184200]
30. Choe KY, et al. , Optogenetic fMRI and electrophysiological identification of region-specific connectivity between the cerebellar cortex and forebrain. Neuroimage, 2018. 173: p. 370–383. [PubMed: 29496611]
31. Chao OY, et al. , Targeting inhibitory cerebellar circuitry to alleviate behavioral deficits in a mouse model for studying idiopathic autism. Neuropsychopharmacology, 2020. 45(7): p. 1159–1170. [PubMed: 32179875]
32. Demirtas-Tatlidede A, et al. , Safety and proof of principle study of cerebellar vermal theta burst stimulation in refractory schizophrenia. Schizophr Res, 2010. 124(1–3): p. 91–100. [PubMed: 20817483]

33. Garg S, et al. , The efficacy of cerebellar vermal deep high frequency (theta range) repetitive transcranial magnetic stimulation (rTMS) in schizophrenia: A randomized rater blind-sham controlled study. Psychiatry Res, 2016. 243: p. 413–20. [PubMed: 27450744]
34. Stoodley CJ and Schmahmann JD, Evidence for topographic organization in the cerebellum of motor control versus cognitive and affective processing. Cortex, 2010. 46(7): p. 831–44. [PubMed: 20152963]
35. Bullitt E, Expression of c-fos-like protein as a marker for neuronal activity following noxious stimulation in the rat. J Comp Neurol, 1990. 296(4): p. 517–30. [PubMed: 2113539]
36. Stewart GR, et al. , N-methylaspartate: an effective tool for lesioning basal forebrain cholinergic neurons of the rat. Brain Res, 1986. 369(1–2): p. 377–82. [PubMed: 3516311]
37. Nitta K, et al. , Minimal Purkinje Cell-Specific PCP2/L7 Promoter Virally Available for Rodents and Non-human Primates. Mol Ther Methods Clin Dev, 2017. 6: p. 159–170. [PubMed: 28828391]
38. Franklin KBJ and Paxinos G, The mouse brain in stereotaxic coordinates, compact third edition. 2008: Academic Press; 3rd edition.
39. Gomez JL, et al. , Chemogenetics revealed: DREADD occupancy and activation via converted clozapine. Science, 2017. 357(6350): p. 503–507. [PubMed: 28774929]
40. Manvich DF, et al. , The DREADD agonist clozapine N-oxide (CNO) is reverse-metabolized to clozapine and produces clozapine-like interoceptive stimulus effects in rats and mice. Sci Rep, 2018. 8(1): p. 3840. [PubMed: 29497149]
41. Yang YM, et al. , Identification of a molecular locus for normalizing dysregulated GABA release from interneurons in the Fragile X brain. Mol Psychiatry, 2020. 25(9): p. 2017–2035. [PubMed: 30224722]
42. Chao OY, Yunger R, and Yang YM, Behavioral assessments of BTBR T+Itpr3tf/J mice by tests of object attention and elevated open platform: Implications for an animal model of psychiatric comorbidity in autism. Behav Brain Res, 2018. 347: p. 140–147. [PubMed: 29545145]
43. Chao OY, et al. , Altered dopaminergic pathways and therapeutic effects of intranasal dopamine in two distinct mouse models of autism. Mol Brain, 2020. 13(1): p. 111. [PubMed: 32778145]
44. Walf AA and Frye CA, The use of the elevated plus maze as an assay of anxiety-related behavior in rodents. Nature Protocols, 2007. 2(2): p. 322–328. [PubMed: 17406592]
45. Aspide R, et al. , Non-selective attention and nitric oxide in putative animal models of Attention-Deficit Hyperactivity Disorder. Behav Brain Res, 1998. 95(1): p. 123–33. [PubMed: 9754884]
46. Kalueff AV, et al. , Neurobiology of rodent self-grooming and its value for translational neuroscience. Nat Rev Neurosci, 2016. 17(1): p. 45–59. [PubMed: 26675822]
47. Milani H, Steiner H, and Huston JP, Analysis of recovery from behavioral asymmetries induced by unilateral removal of vibrissae in the rat. Behav Neurosci, 1989. 103(5): p. 1067–74. [PubMed: 2803554]
48. Simon P, Dupuis R, and Costentin J, Thigmotaxis as an index of anxiety in mice. Influence of dopaminergic transmissions. Behav Brain Res, 1994. 61(1): p. 59–64. [PubMed: 7913324]
49. Ennaceur A and Delacour J, A new one-trial test for neurobiological studies of memory in rats. 1: Behavioral data. Behav Brain Res, 1988. 31(1): p. 47–59. [PubMed: 3228475]
50. Chao OY, et al. , The medial prefrontal cortex - hippocampus circuit that integrates information of object, place and time to construct episodic memory in rodents: Behavioral, anatomical and neurochemical properties. Neurosci Biobehav Rev, 2020. 113: p. 373–407. [PubMed: 32298711]
51. Chaudhuri A, et al. , Molecular maps of neural activity and quiescence. Acta Neurobiol Exp (Wars), 2000. 60(3): p. 403–10. [PubMed: 11016083]
52. Newman ME and Girvan M, Finding and evaluating community structure in networks. Phys Rev E Stat Nonlin Soft Matter Phys, 2004. 69(2 Pt 2): p. 026113. [PubMed: 14995526]
53. Guimera R and Amaral LA, Cartography of complex networks: modules and universal roles. J Stat Mech, 2005. 2005(P02001): p. nihpa35573.
54. Guimera R and Nunes Amaral LA, Functional cartography of complex metabolic networks. Nature, 2005. 433(7028): p. 895–900. [PubMed: 15729348]

55. Kügler S, Kilic E, and Bähr M, Human synapsin 1 gene promoter confers highly neuron-specific long-term transgene expression from an adenoviral vector in the adult rat brain depending on the transduced area. Gene Therapy, 2003. 10(4): p. 337–347. [PubMed: 12595892]
56. Hitti FL and Siegelbaum SA, The hippocampal CA2 region is essential for social memory. Nature, 2014. 508(7494): p. 88–92. [PubMed: 24572357]
57. Smith AS, et al. , Targeted activation of the hippocampal CA2 area strongly enhances social memory. Mol Psychiatry, 2016. 21(8): p. 1137–44. [PubMed: 26728562]
58. Tanimizu T, et al. , Functional Connectivity of Multiple Brain Regions Required for the Consolidation of Social Recognition Memory. J Neurosci, 2017. 37(15): p. 4103–4116. [PubMed: 28292834]
59. Sporns O and Betzel RF, Modular brain networks. Annu Rev Psychol, 2016. **67**: p. 613–40. [PubMed: 26393868] **67**
60. Little JP and Carter AG, Synaptic mechanisms underlying strong reciprocal connectivity between the medial prefrontal cortex and basolateral amygdala. J Neurosci, 2013. 33(39): p. 15333–42. [PubMed: 24068800]
61. Milczarek MM, Vann SD, and Sengpiel F, Spatial memory engram in the mouse retrosplenial cortex. Curr Biol, 2018. 28(12): p. 1975–1980 e6. [PubMed: 29887312]
62. Ranganath C and Ritchey M, Two cortical systems for memory-guided behaviour. Nat Rev Neurosci, 2012. 13(10): p. 713–26. [PubMed: 22992647]
63. Manto M, et al. , Consensus paper: roles of the cerebellum in motor control--the diversity of ideas on cerebellar involvement in movement. Cerebellum, 2012. 11(2): p. 457–87. [PubMed: 22161499]
64. De Zeeuw CI, et al. , Spatiotemporal firing patterns in the cerebellum. Nat Rev Neurosci, 2011. 12(6): p. 327–44. [PubMed: 21544091]
65. Payne HL, et al. , Cerebellar Purkinje cells control eye movements with a rapid rate code that is invariant to spike irregularity. Elife, 2019. 8.
66. Kelly RM and Strick PL, Cerebellar loops with motor cortex and prefrontal cortex of a nonhuman primate. J Neurosci, 2003. 23(23): p. 8432–44. [PubMed: 12968006]
67. Bostan AC and Strick PL, The basal ganglia and the cerebellum: nodes in an integrated network. Nat Rev Neurosci, 2018. 19(6): p. 338–350. [PubMed: 29643480]
68. Insel TR and Fernald RD, How the brain processes social information: searching for the social brain. Annual Review of Neuroscience, 2004. 27: p. 697–722.
69. Simmons DH, et al. , Behavioral tests for mouse models of autism: an argument for the inclusion of cerebellum-controlled motor behaviors. Neuroscience, 2020.
70. Haddon JE and Killcross S, Prefrontal cortex lesions disrupt the contextual control of response conflict. J Neurosci, 2006. 26(11): p. 2933–40. [PubMed: 16540570]
71. Marquis JP, Killcross S, and Haddon JE, Inactivation of the prelimbic, but not infralimbic, prefrontal cortex impairs the contextual control of response conflict in rats. Eur J Neurosci, 2007. 25(2): p. 559–66. [PubMed: 17284198]
72. Gao Z, et al. , A cortico-cerebellar loop for motor planning. Nature, 2018. 563(7729): p. 113–116. [PubMed: 30333626]
73. van Kerkhof LW, et al. , Social play behavior in adolescent rats is mediated by functional activity in medial prefrontal cortex and striatum. Neuropsychopharmacology, 2013. 38(10): p. 1899–909. [PubMed: 23568326]
74. Vanderschuren LJ, Achterberg EJ, and Trezza V, The neurobiology of social play and its rewarding value in rats. Neurosci Biobehav Rev, 2016. 70: p. 86–105. [PubMed: 27587003]
75. Jackman SL, et al. , Cerebellar Purkinje cell activity modulates aggressive behavior. Elife, 2020. 9.
76. Wood M, et al. , Infralimbic prefrontal cortex structural and functional connectivity with the limbic forebrain: a combined viral genetic and optogenetic analysis. Brain Struct Funct, 2019. 224(1): p. 73–97. [PubMed: 30269223]
77. Hughes P, Lawlor P, and Dragunow M, Basal expression of Fos, Fos-related, Jun, and Krox 24 proteins in rat hippocampus. Brain Res Mol Brain Res, 1992. 13(4): p. 355–7. [PubMed: 1320724]

78. Luckman SM, Dyball RE, and Leng G, Induction of c-fos expression in hypothalamic magnocellular neurons requires synaptic activation and not simply increased spike activity. J Neurosci, 1994. 14(8): p. 4825–30. [PubMed: 8046453]

79. Guell X, Gabrieli JDE, and Schmahmann JD, Triple representation of language, working memory, social and emotion processing in the cerebellum: convergent evidence from task and seed-based resting-state fMRI analyses in a single large cohort. Neuroimage, 2018. 172: p. 437–449. [PubMed: 29408539]

80. Guell X, et al. , Functional gradients of the cerebellum. Elife, 2018. 7.

81. Zeidler Z, Hoffmann K, and Krook-Magnuson E, HippoBellum: acute cerebellar modulation alters hippocampal dynamics and function. J Neurosci, 2020. 40(36): p. 6910–6926. [PubMed: 32769107]

82. King M, et al. , Functional boundaries in the human cerebellum revealed by a multi-domain task battery. Nat Neurosci, 2019. 22(8): p. 1371–1378. [PubMed: 31285616]

83. Schmahmann JD, Weilburg JB, and Sherman JC, The neuropsychiatry of the cerebellum - insights from the clinic. Cerebellum, 2007. 6(3): p. 254–67. [PubMed: 17786822]

84. Wang SS, Kloth AD, and Badura A, The cerebellum, sensitive periods, and autism. Neuron, 2014. 83(3): p. 518–32. [PubMed: 25102558]

85. Andreasen NC and Pierson R, The role of the cerebellum in schizophrenia. Biol Psychiatry, 2008. 64(2): p. 81–8. [PubMed: 18395701]

86. Diener HC and Dichgans J, Pathophysiology of cerebellar ataxia. Mov Disord, 1992. 7(2): p. 95–109. [PubMed: 1584245]

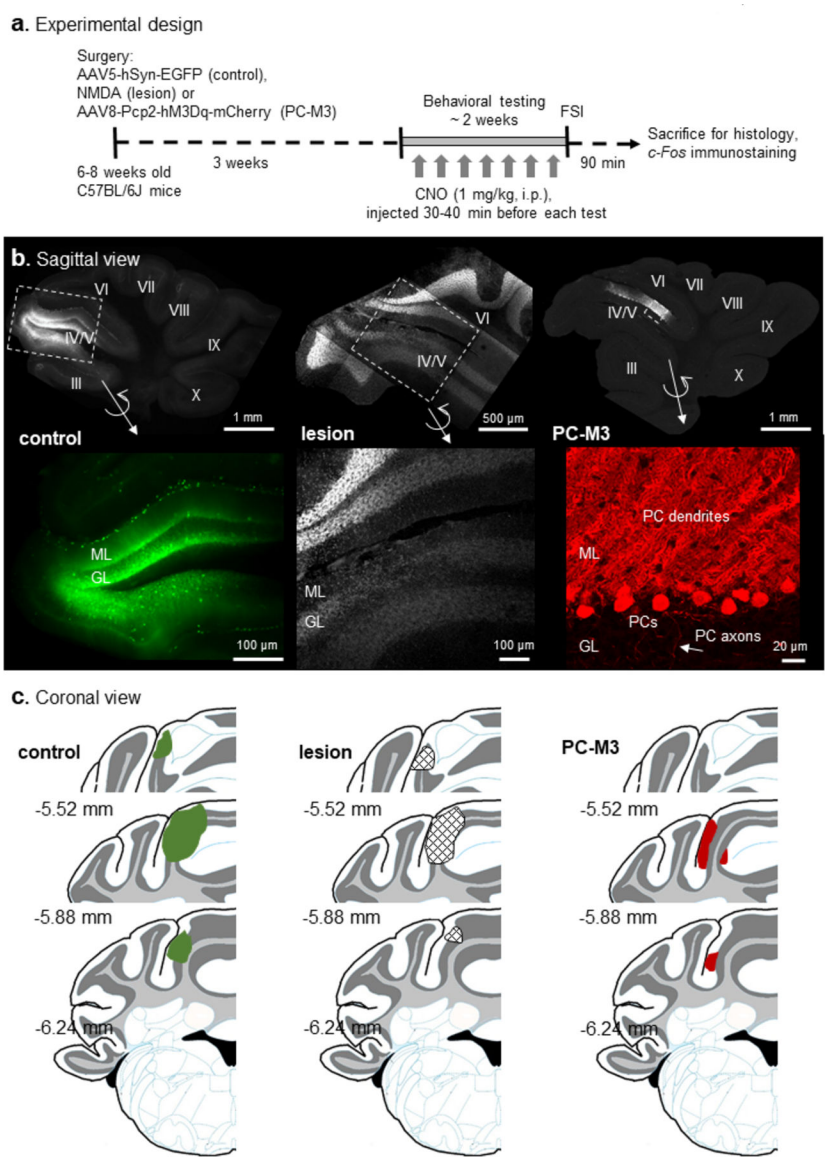

Fig 1. Experimental design and histological examination.

(**a**) Mice were randomly divided into AAV5-hSyn-EGFP (control), NMDA (lesion) and AAV8-Pcp2-hM3Dq-mCherry (PC-M3) groups, followed by a series of behavioral tests. Clozapine-*N*-oxide (CNO, 1 mg/kg) was given to all the groups before each test. Mice were sacrificed 90 min after the final test (free social interaction, FSI) and *c-Fos* immunostaining was performed. (**b**) Examples of the sagittal view of cerebellar slices from the control, lesion and PC-M3 groups. Fluorescence in lobule IV/V was EGFP (control), DAPI (lesion) or mCherry (PC-M3). Zoom-in images are shown in bottom panels. In the control group, EGFP was found preferentially in granule cells and interneurons. In the lesion group, cell loss was seen in molecular layer (ML), Purkinje cell (PC) layer, and granular layer (GL). In the PC-M3 group, only PCs were labelled with mCherry. (**c**) Diagrams of the coronal view of cerebellar sections. Affected areas in lobule IV/V are highlighted in green (EGFP

in control group), grid-shaped (lesions in lesion group) and red (mCherry in PC-M3 group), respectively. Numbers indicate distance relative to the bregma.

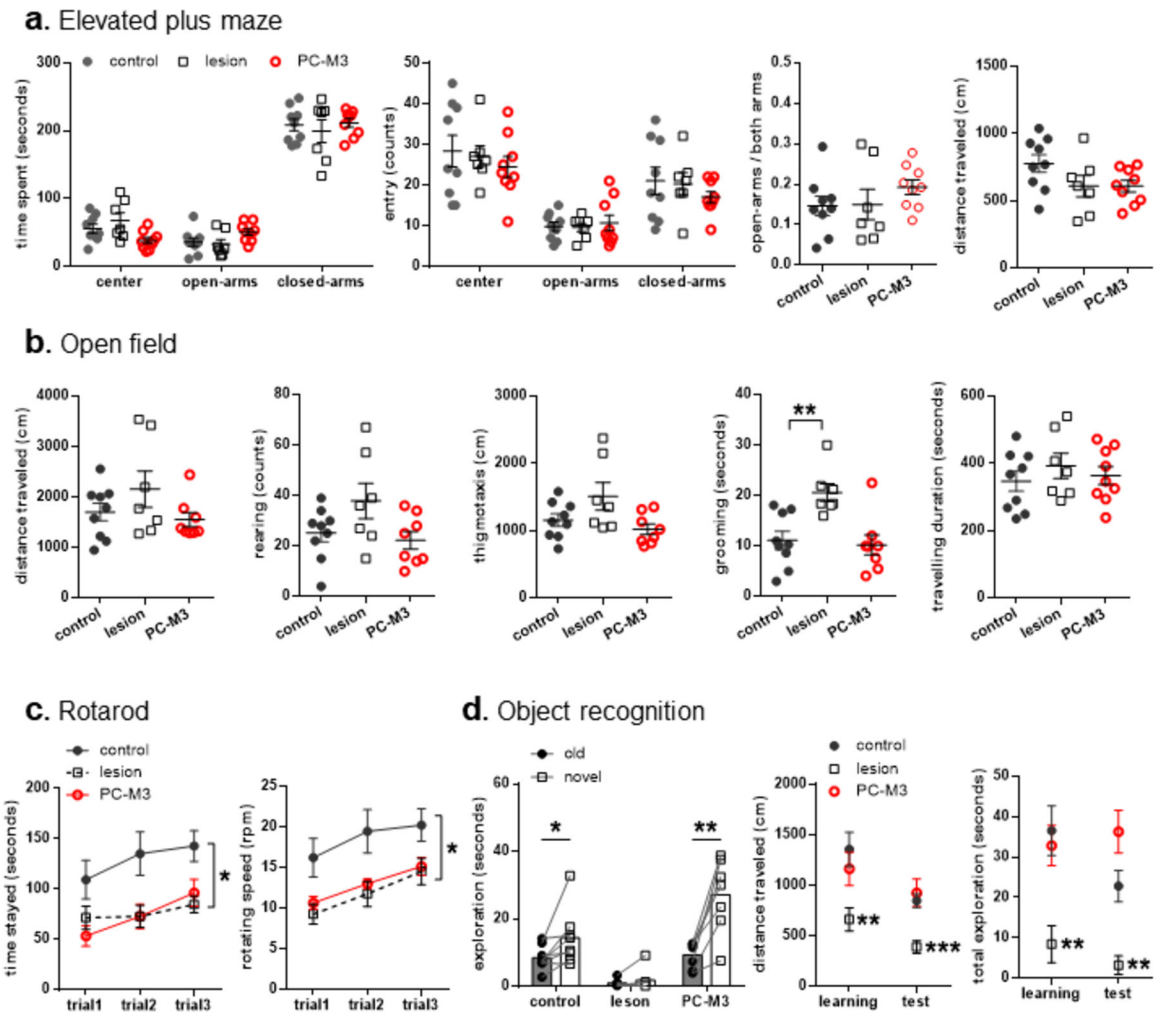

Fig 2. Effects of lesion or chemogenetic excitation of PCs in lobule IV/V on anxiety-related behavior, locomotor activity, motor coordination and object memory.

(**a**) No significant differences were found between control and lesioned or PC-M3 animals in the elevated plus maze. (**b**) In the open field, the lesion group had more self-grooming than the controls, while both lesion and PC-M3 groups showed comparable locomotor activities to the controls. (**c**) The lesion and PC-M3 groups displayed impaired motor coordination on an accelerating rotarod. (**d**) The control and PC-M3 groups showed intact object memory, but the lesion group did not. The lesioned animals also exhibited less motor activity and exploration of the objects than the controls. n=7–9/group. Values are shown as mean ± SEM. *p<0.05, **p<0.01, ***p<0.001, compared to the control group or respective values.

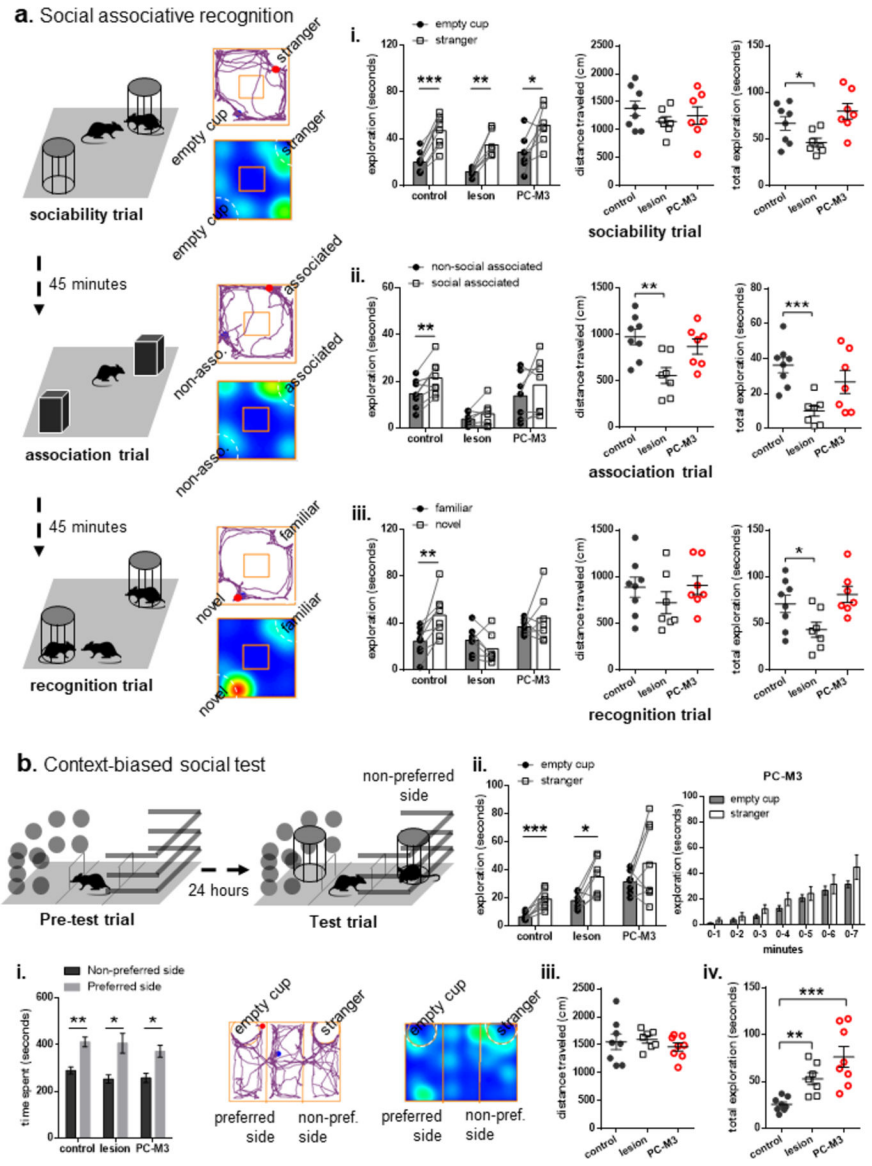

Fig 3. Lesion or chemogenetic manipulation in lobule IV/V disrupted social behaviors.

(**a**) Illustration of the social associative recognition test, including three trials: sociability (exploration of a stranger and an empty cup), association (exploration of two identical objects, placed at the same locations of the previously explored stimuli) and recognition (exploration of the previously encountered stranger and a novel stranger). Examples of movement tracking (blue and red dots indicate the start and end points, respectively) and heat-map of time spent (the spectra from red to blue represents long to short duration) from a control animal were presented. (i) All the groups explored the stranger more than the empty cup in the sociability trial, while the lesion group had less total exploration. (ii) Only the control group explored the associated object more than the non-associated object in the association trial. The lesioned animals had less distanced travelled and total exploration than the controls. (iii) Only the control group explored the novel stranger more than the familiar one. The lesion group again showed less total exploration than the control

group. (**b**) Diagram of the context-biased social test: exploration of the three-chambered box with two distinct contexts (pre-test trial), followed by exploration of a stranger located in the non-preferred side and an empty cup located in the other side (test trial). (i) All the groups formed a natural contextual preference in the pre-test trial. An example of movement tracking and heat-map of time spent from a control animal in the test trial was presented. (ii) In the test trial, the control and lesion groups explored the stranger located in the non-preferred context more than the empty cup located in the preferred context, while the PC-M3 group did not across time periods of the test. (iii) No group difference was found in distance travelled in the test trial. (iv) Yet, the lesion and PC-M3 groups had higher total exploration than the control group. n=7–8/group. Values are shown as mean ± SEM. *p<0.05, **p<0.01, ***p<0.001, compared to the control group or respective values.

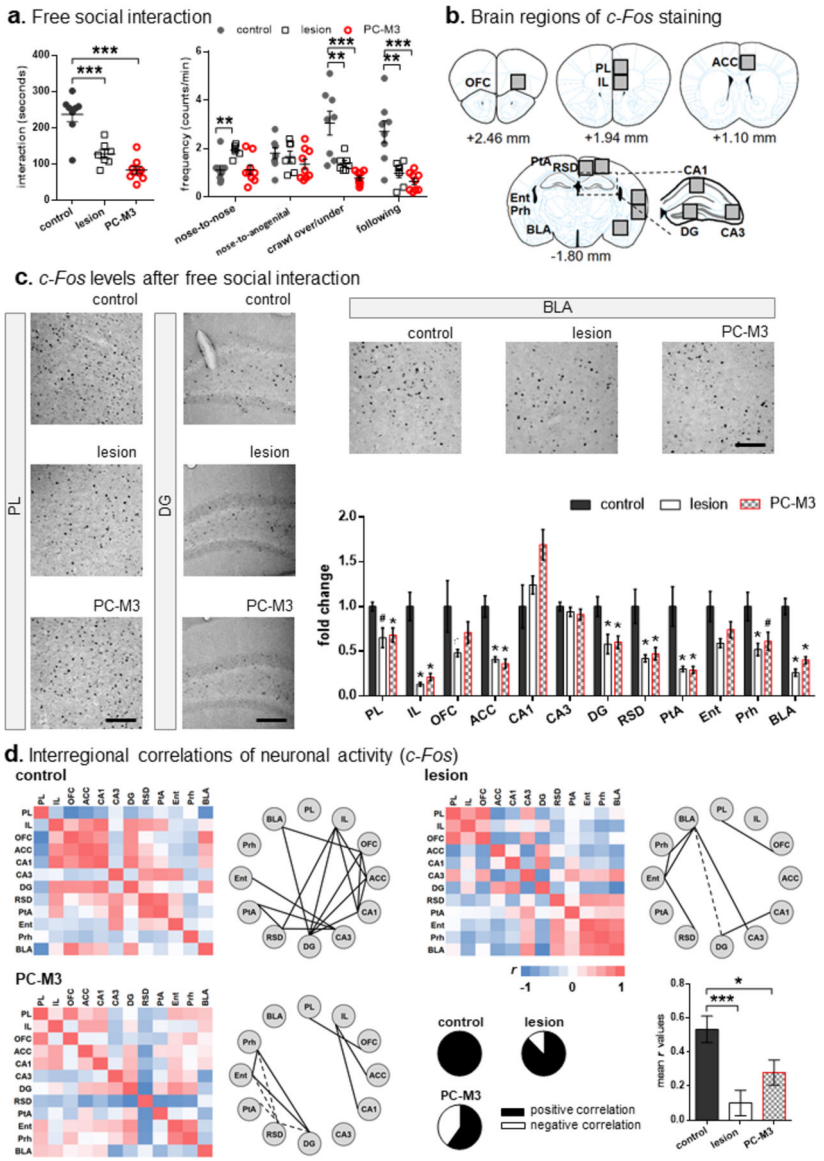

Fig 4. Lesion or chemogenetic manipulation in lobule IV/V reduced free social interaction and *c-Fos* levels in multiple brain regions.

(**a**) The lesion and PC-M3 groups displayed less social interaction and lower frequencies of crawling and following behaviors than the control group. The lesioned mice had more nose-to-nose/head contacts than the controls. n=7–9/group. (**b**) Brain regions imaged for *c-Fos*-positive cells. Numbers indicate mean distance relative to the bregma in ± 0.1–0.2 mm range. (**c**) Examples of *c-Fos* images in the PL, DG and BLA, and fold change of *c-Fos*-positive cells measured across the brain regions. Scale bars: 50 μm. The lesion and PC-M3 groups showed fewer *c-Fos* signals in the PL, IL, ACC, DG, RSD, PtA, Prh and BLA than the control group. n=5–6/group. (**d**) Matrices of interregional correlations for *c-Fos*-positive cells and significant connections (solid and dash lines represent positive and negative correlations, respectively) in the three groups. Relative proportions of positive and negative correlations for each group are shown in the pie charts. The lesion and PC-M3 groups had lower average correlations *r* than the control group in the calculation of all

interregional correlation coefficients. Values are shown as mean ± SEM. *p<0.05, **p<0.01, ***p<0.001, #p=0.052, compared to the control group. PL: prelimbic cortex; IL: infralimbic cortex; OFC: orbitofrontal cortex; ACC: anterior cingulate cortex; DG: dentate gyrus; RSD: dorsal retrosplenial cortex; PtA: parietal association cortex; Ent: entorhinal cortex; Prh: perirhinal cortex; BLA: basolateral amygdala.

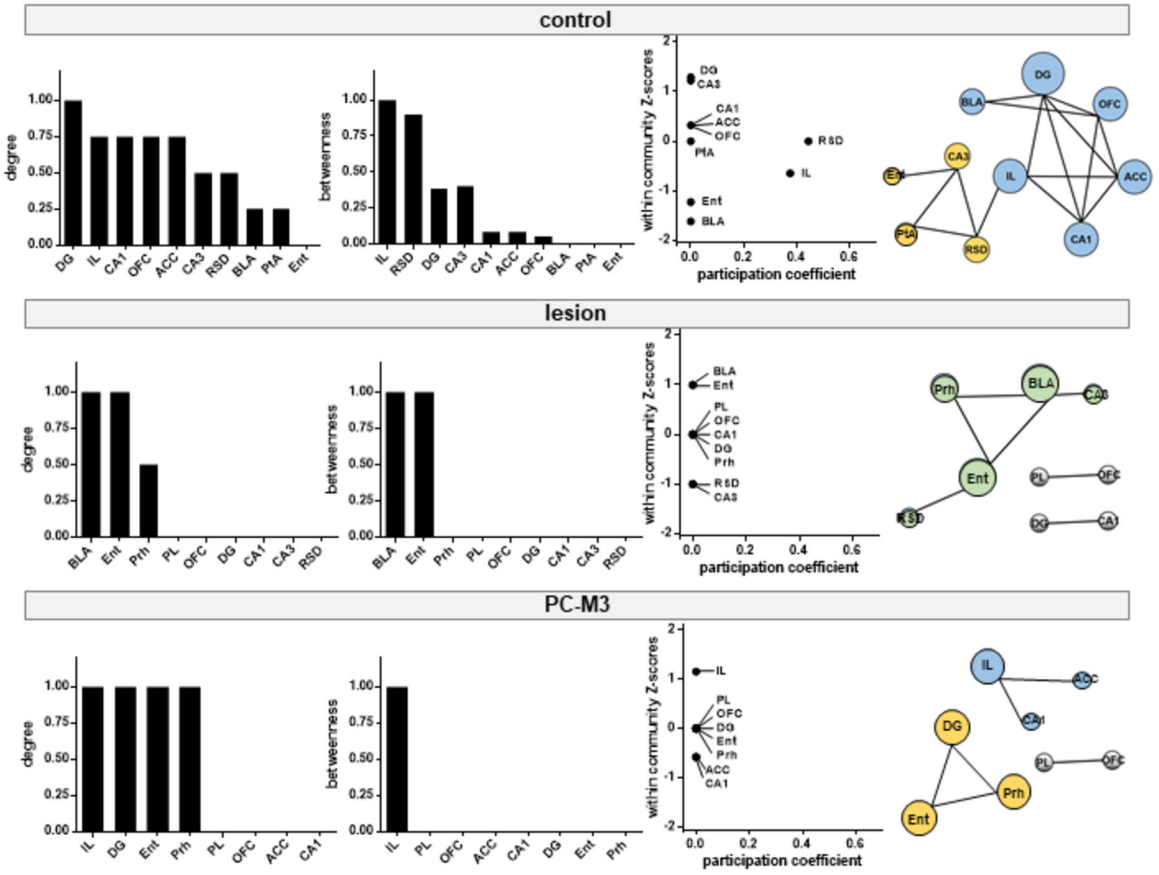

Fig 5. Lesion or chemogenetic perturbation of lobule IV/V disorganized neural networks required for free social interaction.

Brain hubs identified by graph theoretical analysis of the networks activated following free social interaction. Normalized degree and betweenness are ranked in descending order for each group. Neuronal modules are identified via modularity maximization, based on within-community Z-scores and participation coefficients for each brain region. Different modules are color-coded and the size of nodes (brain regions) is proportional to their degree in the network. PL: prelimbic cortex; IL: infralimbic cortex; OFC: orbitofrontal cortex; ACC: anterior cingulate cortex; DG: dentate gyrus; RSD: dorsal retrosplenial cortex; PtA: parietal association cortex; Ent: entorhinal cortex; Prh: perirhinal cortex; BLA: basolateral amygdala.

Table 1.

Time spent (seconds) in each chamber in the test trial of context-biased social test. Values are shown as mean ± SEM.

	center	cup side	stranger side
control	67.68 ±9.43	156.50 ±22.67	195.84 ±20.99
lesion	115.17 ±12.41 **	160.31 ±20.42	143.59 ±12.79
PC-M3	105.90 ±16.42	166.48 ±16.77	145.91 ±25.27

** $p<0.01$, compared to controls.

Table 2.

Summary of behavioral effects of NMDA-induced lesions (lesion) or chemogenetic excitation of Purkinje cells (PC-M3) in cerebellar lobule IV/V.

	lesion		PC-M3	
Elevated plus maze	---		---	
Rotarod	**X**		**X**	
Open field	---	high grooming	---	
Object recognition	**X**	low activity	---	
		low exploration		
Social associative recognition				
sociability	---	low exploration	---	
social association	**X**	low activity	**X**	
		low exploration		
social recognition	**X**	low exploration	**X**	
Context-biased social test				
context preference	---		---	
context-biased sociability	---	high exploration	**X**	high exploration
Free social interaction	**X**		**X**	

---: No effect compared to controls; X: deficient effect compared to controls.